Published in final edited form as:
Hippocampus. 2014 September ; 24(9): 1129–1145. doi:10.1002/hipo.22297.

Cognitive Impairment in Temporal Lobe Epilepsy: Role of Online and Offline Processing of Single Cell Information

A. S. Titiz[1,*], **J. M. Mahoney, PhD**[1,2,3], **M. E. Testorf, PhD**[1,4], **G. L. Holmes, MD**[1,3], and **R. C. Scott, MD PhD**[1,3,5]

[1]Department of Neurology, Geisel School of Medicine at Dartmouth, Hanover, New Hampshire

[2]Department of Genetics, Geisel School of Medicine at Dartmouth, Hanover, New Hampshire

[3]Department of Neurological Sciences, University of Vermont College of Medicine, Burlington, Vermont

[4]Thayer School of Engineering, Dartmouth College, Hanover, New Hampshire

[5]Institute of Child Health, UCL, London, United Kingdom

Abstract

Cognitive impairment is a common comorbidity in temporal lobe epilepsy (TLE) and is often considered more detrimental to quality of life than seizures. While it has been previously shown that the encoding of memory during behavior is impaired in the pilocarpine model of TLE in rats, how this information is consolidated during the subsequent sleep period remains unknown. In this study, we first report marked deficits in spatial memory performance and severe cell loss in the CA1 layer of the hippocampus lower spatial coherence of firing in TLE rats. We then present the first evidence that the reactivation of behavior-driven patterns of activity of CA1 place cells in the hippocampus is intact in TLE rats. Using a template-matching method, we discovered that real-time (3–5 s) reactivation structure was intact in TLE rats. Furthermore, we estimated the entropy rate of short time scale (~250 ms) bursting activity using block entropies and found that significant, extended temporal correlations exist in both TLE and Control rats. Fitting a first order Markov Chain model to these bursting time series, we found that long sequences derived from behavior were significantly enriched in the Markov model over corresponding models fit on randomized data confirming the presence of replay in shorter time scales. We propose that the persistent consolidation of poor spatial information in both real-time and during bursting activity may contribute to memory impairments in TLE rats.

Keywords

place cells; replay; Markov chain; sleep; reactivation

[*]**Corresponding Author:** Ali S. Titiz titiz@dartmouth.edu 564E Borwell Building Dartmouth-Hitchcock Medical Center One Med Ctr Drive Lebanon, NH 03766.

Author contributions: AST designed experiments and collected data. GLH and RCS supervised the project. AST, JMM, and MET developed and implemented the template-matching algorithm. AST and JMM developed and implemented the Markov Chain model analyses. AST and RCS conducted statistical analyses. AST prepared the manuscript with review support from RCS and GLH. All authors discussed the results and implications and commented on the manuscript at all stages.

Introduction

Temporal lobe epilepsy (TLE) is the most common epilepsy syndrome occurring in adults (Tellez-Zenteno and Hernandez-Ronquillo, 2012). Cognitive impairments are common in patients with TLE (Jokeit et al., 2000; Strauss et al., 1995; Vlooswijk et al., 2010) and may even persist with sufficient control of seizures. While the pathological features of severe neuronal cell loss and gliosis in the hippocampus have been described (Mathern et al., 1996), the mechanism by which TLE pathology relates to cognitive impairment has not been well established. Coincidentally, sleep disorders are common comorbidities in patients with TLE (Dewolfe et al., 2013; Herman, 2006; Malow, 2007) which, considering the role of sleep in memory performance improvements (Diekelmann and Born, 2010; Stickgold, 2005; Stickgold et al., 2002; Walker and Stickgold, 2004; Walker and Stickgold, 2006; Walker and Stickgold, 2010), may further exacerbate cognitive impairments.

The hippocampus is considered to play a crucial role in the formation of long-term memories in humans (Manns et al., 2003a; Manns et al., 2003b; Miller et al., 1998; Scoville and Milner, 1957; Zola-Morgan et al., 1986) as well as spatial memory in rodents (Morris, 1984; O'Keefe and Dostrovsky, 1971) and it is severely affected in TLE in humans (Bernasconi et al., 2003; Tellez-Zenteno and Hernandez-Ronquillo, 2012) and rats (Curia et al., 2008; Matos et al., 2010; Sharma et al., 2007). The lithium-pilocarpine model of TLE in the rat is associated with marked cell loss in the hippocampus (Clifford et al., 1987; Mello et al., 1993; Wu et al., 2001). Studies of the hippocampus in TLE rats have shown evidence of poor spatial processing at the levels of behavior (Holmes and Lenck-Santini, 2006; Kleen et al., 2012; Lin et al., 2009; Liu et al., 1994), oscillations (Kleen et al., 2011; Lenck-Santini and Holmes, 2008; Richard et al., 2013) and single-units (Lenck-Santini and Holmes, 2008; Liu et al., 2003; Scott et al., 2011; Tyler et al., 2012; Zhou et al., 2007). A candidate mechanism for sleep-related improvements in memory performance is the experience-dependent reactivation of place cell activity patterns representative of previous behavior—previously defined as hippocampal replay (Davidson et al., 2009; Lee and Wilson, 2002; Louie and Wilson, 2001; Nadasdy et al., 1999; Wilson and McNaughton, 1994). Replay was discovered to occur both during high-frequency ripple oscillations (Buzsaki, 1989; Diba and Buzsaki, 2007; Jackson et al., 2006) where many hippocampal neurons are activated in close temporal proximity (Davidson et al., 2009; Ji and Wilson, 2007; Lee and Wilson, 2002; Wilson and McNaughton, 1994) as well as in real-time during NREM (Ribeiro et al., 2004; Ribeiro et al., 2007) and REM sleep periods (Louie and Wilson, 2001). In this study, we consider replay in both real-time and bursting activity (~250 ms) time scales in TLE rats.

Both behavioral (Bazil and Walczak, 1997; Malow, 2007) and electrographic (Fernandez et al., 2012) manifestations of TLE are modulated by sleep states (Crespel et al., 1998; Crespel et al., 2000) raising the possibility that abnormalities in sleep architecture may contribute to memory impairments in TLE (Chan et al., 2011). Previous studies show that TLE rats have poor spatial memory performance (Liu et al., 1994) accompanied by decreased place field stability and increased out-of-field firing of hippocampal place cells (Liu et al., 2003) which indicate poor memory encoding in the hippocampus at the single-cell level. The study of replay during sleep in TLE rats, however, has remained a challenge due to technical difficulties in recording multiple neurons in the damaged CA1 layer simultaneously.

Moreover, the impact of pathology on systems important for memory consolidation remains relatively unexplored and their examination may improve upon the current understanding of basic memory processing. A recent study (Suh et al., 2013) reported that the sequential reactivation of place cells during sharp-wave ripple (SWR) events were completely abolished in a mouse model of schizophrenia. Thus, studying memory processes in disease states may be valuable in providing information about how the hippocampal system responds to perturbation by disease. We hypothesize that the reactivation of behavior-related patterns of neural activity is disrupted in TLE rats both during bursting activity and in real-time.

Here, we report the first evidence that behavior-driven sequences of single-unit activity in the subsequent rest period is significantly enriched in first-order Markov Chain models of the single unit bursting activity during rest. In fact, our block entropy analyses show that a large portion of the information in the resting period is contained in pairwise relationships between burst events. Moreover, the behavior sequences are significantly more probable in the first order Markov Chain model than corresponding models of randomized data indicating that the temporal structure during the resting period is enriched for longer, behaviorally relevant sequences. Thus, knowing the place cell that has just fired is highly predictive of the next place cell to be activated within a replay event in both the TLE and control groups of rats. This chain of activity during the bursting activity may sustain long-term firing relationships following Hebbian rules for synaptic plasticity (Hebb, 1949).

The TLE rats in this study exhibited severe histopathological abnormalities in the hippocampus paired with marked spatial memory deficits. We further show spatial processing deficits in the single-cell level. In consideration of how sleep-related memory processing mechanisms may be affected in TLE rats, we report robust presence of reactivation structure in real-time (3–5 s) and replay in short-time (~250 ms) bursting activity.

Materials and Methods

Seizure Induction

The lithium-pilocarpine model of status epilepticus was used to create animals with temporal lobe epilepsy (N=3). Sprague-dawley rats were injected with lithium chloride (3 mg/kg) intraperitoneally (i.p.) 18 h before pilocarpine injections on postnatal day (P) 40. Thirty minutes before the pilocarpine injection, rats received a subcutaneous injection of methyl-scopolamine (1 mg/kg), a muscarinic cholinergic receptor antagonist, to prevent systemic cholinergic effects. Pilocarpine injections (10 mg/kg) were performed every 30 min until the first signs of seizures were observed as previously reported by our group (Richard et al., 2013). Seizures were stopped using isoflurane (3% for 1 h) one hour after rats enter status by standing on their hind legs and falling on their backs. Another group of animals were given normal saline i.p. 18 h before an additional saline injection at P40. Control and TLE animals were handled similarly. Only TLE rats with at least one unprovoked seizure observed at least two weeks after induction were included in this study.

Morris Water Maze Task

The Morris water maze task was used to study spatial learning and memory in rats with TLE and controls (Morris, 1984). In this task, a platform (diameter= 10 cm, height = 48.5 cm) was submerged into a tub (diameter = 2 m; height = 50 cm) of opaque water with distal cues around the tub. The platform was placed at 9 o'clock, 33 cm away from the wall of the tub. The walls in the room around the water maze were covered with black cloth to create a covered area of 4-by-6 m. Two distal cues (one white background with a black “X” in the middle and another with a black and white pattern) were placed on the black cloth covering the walls 50 cm away from the edge of the water maze at 11 o'clock and 2 o'clock, respectively. Indirect lighting was provided with three 20 W spotlights placed on the floor near the water maze and were directed at the distal cues. The animals were placed into the water from different locations at the beginning of each trial and their latency to finding the platform was timed. The decrease in latency was studied as a proxy for spatial learning ability. The animals performed 4 trials per session per day over 5 days. A 2-minute probe trial, where the platform was removed, was performed on the last day immediately following the last set of trials and time spent in target quadrant (i.e., where the platform is placed) and non-target quadrants measured.

Screening and Recording

The signal from the electrodes was amplified by a series of operational amplifiers and transited through cable attached to a rotating commutator that allowed the rat to move freely. Tetrode signal was amplified ×10'000 with low-noise differential amplifiers. The data acquisition system, Digitalynx (Neuralynx, Bozeman, MT), recorded a 1 ms burst of 32 samples at 32 kHz whenever the voltage exceeds a manually determined threshold. The EEG signal was band-pass filtered at 0.1–30 Hz and the EMG signal was band-pass filtered at 10–50 Hz for visual analysis. A light-emitting diode (LED) was placed on the rat head-stage in order to track the rat's position via a CCD camera at 30 Hz. A week after surgery, the signal from the electrodes was monitored 3 times daily for waveforms of sufficient amplitude. If no waveform of sufficient amplitude was detected, electrodes were advanced by increments of 50 μm and a minimum of 4 hours was allowed before proceeding to the next screening. Unit discrimination was done using cluster-cutting software (SpikeSort 3D; Neuralynx, Bozeman, MT). Only units with peak spike amplitude over 100 μV on at least one tetrode wire were included. All following analyses were performed using MatLab (Mathworks, Natick, MA). The pyramidal cells were identified from their firing rates and waveforms with interspike intervals lower than 5 ms, an average firing rate less than 3 Hz, 10 Hz peak in-field firing rates and peak-to-through time lags between 300–500 μs. From cells that fulfill these criteria, pyramidal cells were determined as place cells based on the presence of a place field that was more than 9 contiguous pixels with a firing rate at least three times greater than their session average on their rate maps (Muller and Kubie, 1987). Spatial coherence scores were calculated as two-dimensional nearest-neighbour autocorrelation of each place cell's firing rate within a 1 cm × 1 cm pixel with its eight nearest neighbours to estimate the spatial fidelity of firing within a place field (Zhou et al., 2007). Electrodes were moved 25–100 μm between experiments in order to sample from a new population of place cells.

Circular Track Task

TLE rats (number of rats N=3; number of experiments n=5) and controls (N=3; n=6) were trained to run in a circular track for food reward. An experiment was defined as a 20 minute spatial memory performance in the circular track followed by 1 h rest period. Electrophysiological data was collected throughout the experiment both during performance and the rest periods. Each animal's directional preference (clockwise or counter-clockwise) during training sessions was reinforced to promote movement in the maze in the preferred direction in an effort to decrease training time. Incorrect or incomplete turns were not rewarded. Animals were required to complete 20 correct turns in 15 min to be included in the study. After training, single-unit and local EEG activity were recorded while animals performed >20 turns in 15 minutes (RUN). Afterwards, the animals were placed in their home cages above the center of the circular track and their single-unit, EEG, and EMG activity were recorded for 1 hour (POST).

Computation of the Consensus Templates

The amount of time taken by each animal to complete a turn varied between and within animals. This observation required the construction of cell activity patterns normalized over time to account for differences in the time lags between place cells due to the speed of the animal. This method was preferred over decoding by space due to the observation that not all place cells fired in each turn, a phenomenon previously reported (Fenton et al., 2010). Thus, decoding my space may have placed neurons in sequences that do not occur in the real data. To construct a template of RUN temporal activity, we took each of the RUN epochs and computed their correlation coefficient profile across the whole behavior recording. These profiles show peaks during the RUN epochs, with a maximum peak of 1 when the template is compared to the epoch from which it was taken. These peak profiles were aligned to each other by identifying the lag of maximum cross-correlation of the peaks. The lags are the distances that the peaks are shifted with respect to each other across different RUN epochs (e.g. the rat might pause briefly before entering the maze, thus causing a lag in the appearance of the RUN template). The pairwise optimal lags do not necessarily have to agree with each other; two profiles might optimally align at zero-lag, but disagree about their lag with respect to a third profile. To address this heterogeneity, we computed the average lag distance between templates and rounded to the nearest time bin.

In addition to the cross-correlation heterogeneity, there is heterogeneity in the speed with which the rats traverse the maze. Nevertheless, the rats move at roughly constant speed and so the temporal ordering of their cell activity is preserved, while their bursts may be stretched or squeezed in time with respect to each other. To account for this, the rasters from each RUN epoch were standardized to the median of the RUN time for the rat. Specifically, the spike times were compressed or expanded by a factor determined by the ratio of RUN epoch to the median duration of the RUN epochs. This standardized time allows for direct comparisons between peak profiles.

Consensus templates representing time-dependent firing properties of units were constructed by compiling pyramidal cell spiking activity during all correct turns during RUN and smoothing their spikes with a Gaussian function (σ=1 s, binned at 10 ms). The smoothed

rasters were then aligned by determining the maximum cross correlation (within one template distance) of their correlation coefficient profiles as an offset. The shifted templates were then averaged to determine the consensus alignment of the smoothed profiles. The consensus template was used as a cohesive representation of firing probability for each place cell over a normalized time period (3±1.5 s) where the animals took an average of ~3 s to complete a turn. Both groups of animals required similar temporal scaling to fit the behavior data.

Template-Matching Method

A template matching method was used to investigate real-time temporal structure in the firing patterns of cell ensembles as described in (Louie and Wilson, 2001). Cell activity was recorded simultaneously from a (*C*) number of cells during sleep and the resulting matrix of cell activity over time is compared to consensus templates over moving windows of an (*N*) length as shown in Equation 1 (Louie and Wilson, 2001). The sleep period is binned at 10 ms to ensure a high temporal resolution where x_{1C}, x_{2C},…,X_{NC} is the smoothed consensus templates and y_{1C}, y_{2C},…,y_{NC} are the binned sleep dataset. $\bar{x}$ and $\bar{y}$ are mean bin values with standard deviations σ_x and σ_y, respectively. The consensus sequence was compared to the entire sleep period where template correlation coefficients (C_t) were calculated over overlapping moving windows centered at time *t*. The resulting correlation coefficient vector was then z-scored against 100 vectors of the same size calculated using the corresponding shuffled data.

$$C_t = \frac{\frac{1}{N \cdot C} \sum_{c=1}^{C} \sum_{n=1}^{N} \left(\frac{x_{nc}}{X_c} - \bar{x} \right) \left(\frac{y_{nc}}{Y_c} - \bar{y} \right)}{\sigma_x \sigma_y} \quad \text{(Equation 1)}$$

where,

$$X_c = \sqrt{\frac{1}{N} \sum_{n=1}^{N} X_{nc}^2}$$

$$\bar{x} = \frac{1}{N \cdot C} \sum_{c=1}^{C} \sum_{n=1}^{N} \frac{X_{nc}}{X_c}$$

$$\sigma_{x,y} = \sqrt{\frac{1}{N \cdot C} \sum_{c=1}^{C} \sum_{n=1}^{N} \left(\frac{x_{nc}}{X_c} - \bar{x} \right)^2}$$

Shuffling Method for a Null Distribution in Real-Time

In order to compare results from the template matching method using real datasets, null distributions were constructed by shuffling unit activity during POST. For all shuffling procedures, sleep states were shuffled separately to control for the possibility that stochastic

activity in NREM sleep may perturb structure in other states if shuffled together. We used a column shuffling method where activity of all neurons in 10 ms bins are shuffled across time to preserve zero-lag relationships within firing patterns. We compared Ct measurements from real data using the null distribution provided by this shuffling method to test the hypothesis that patterns of activity during behavior are reactivated in real-time in the subsequent rest period.

Markov Chain Model

Following the finding that real-time reactivation was preserved in TLE rats, we asked whether reactivation could be observed on a shorter time scale during population bursts. Population bursts were defined as cell activity flanked by absence of all cell activity for at least 100 ms (Davidson et al., 2009; Ji and Wilson, 2007; Suh et al., 2013). The firing activity contained between these silent periods was parsed into separate groups (words) and each cell's activity within each word was represented by its median time of firing. We have also conducted the same analyses using visually picked peaks for each cell during behavior in order to account for cells with multiple place fields. We elected to present data with median firing rates as this analysis yielded the same results and for the sake of consistency. We then transformed the sequences obtained using this method into transition matrices of first order Markov Chains by counting the number of transitions between pairs of cells in a cell × cell matrix and normalizing by the row sums of the matrix (Fig. 7b), which yields the probability (p_{ij}) of transitions from one cell (i) to the next (j) in a given sequence from order X_n to X_{n+1} as shown in Equation 2 (Markov, 1971).

$$\mathrm{p}_{ij}=Pr\left(\mathrm{X}_{\mathrm{n}+1}=\mathrm{j}|\mathrm{X}_{\mathrm{n}}=\mathrm{i}\right) \quad \text{(Equation 2)}$$

Shuffling Method for the Null Distribution for the Markov Chain Model

The null distributions for the Markov Chain analyses were obtained by shuffling unit identities between non-silent periods where word lengths and total number of observations for each unit are preserved. The null distribution obtained using this method tests the hypothesis that the sequences observed in the real dataset have high correlations between symbols--i.e., they are more correlated than suggested by independent firing.

Statistical Analyses

Data were analyzed using SPSS (IBM Corporation, Armonik, NY), STATA (Statacorp, College Station, TX) and custom software developed in MatLab (Mathworks, Natick, MA). The histological scoring data was compared using t-tests comparing cell loss and mossy fiber sprouting in each region. Data are presented as mean ± SEM. Water maze data was first analyzed using Cox proportional hazards model in STATA where latency data was modeled with trials, days, and animals in repeated measures. The goodness of fit of the Cox Regression model was evaluated with a test of the proportional-hazards assumption using Schoenfield residuals (p=0.9710). Trial-by-trial analysis of the water maze data was conducted using repeated measures ANOVA. Time spent in each quadrant was analyzed using t-tests to test for differences between the groups in time spent in each quadrant. We used Generalized Estimating Equations (GEE) to model the effect of TLE on place cell

coherence, behavioral performance measures, average firing rates of cells and histological scoring(Lucas et al., 2011; Richard et al., 2013; Tyler et al., 2012). GEE is a class of regression marginal model for investigating the relationships between clustered response data and outcome measures in a multivariable manner. Units' firing rate and time spent in sleep stages were compared using GEE modeling the effect of stage (RUN or POST) and state (Awake, NREM sleep, REM sleep) on firing rate and proportion of time spent in each state, respectively.

Template-correlation results were analyzed using custom software developed in MatLab (Mathworks, Natick, MA). Single-unit data collected for each animal was binned at 10 ms and shuffled using methods outlined above for each unit. The template correlation analysis was then conducted by correlating the consensus templates obtained from real data and with the shuffled dataset. This process was repeated 100 times for the shuffled datasets and the resulting shuffled correlation vectors were concatenated into a vector to be used as a null distribution. Z-scores were calculated for the real dataset using the shuffled null distribution. Two-sample Kolmogorov-Smirnov (KS) tests were used to differences between the real and the null distribution for each experiment as well as the two groups of rats. The 95^{th} percentiles of the corresponding null distributions were used to threshold the datasets to compare the weights of z-scores at the 95^{th} percentile tails (sum of z-scores above 1.96) of the distributions of each animal to its null. This approach enabled us to ask whether there was real-time structure in real data that cannot be explained by chance alone. The Markov Chain approach was analyzed using a shuffled null distribution where word lengths and firing rates were preserved. Specifically, a full burst sequence was formed from the burst words by concatenating them, but separated by a special character “0” to indicate a period of silence. This full sequence was randomly permuted with the 0's fixed in order to preserve the distribution of lengths of words and the bursting rates of neurons. This was repeated 1000 times to obtain a null distribution with which the behavior sequence probability was z-scored. In order to study whether there was high-order structure in the dataset, we employed a Block Entropy approach where we calculated the entropy of k-grams within words for each experiment in each state (for k=1–8) using an entropy estimator (Nemenman et al., 2001).

Electrode Preparation

32-channel multi-electrode arrays were implanted into the hippocampus. The multielectrode array we used is manufactured in Robert U. Muller's Laboratory (State University of New York, Downstate Medical Center, Brooklyn, NY). The multi-electrode arrays were composed of seven independently movable tetrodes and one 100 μm single-wire electrodes for local EEG recordings. For the tetrodes, 25 μm nichrome wires (A-M Systems, Sequim, WA) were assembled, twisted in a tight bundle, and then run through polymicrotubing (Neuralynx, Bozeman, MT). Two additional 0.25 mm stainless steel wires extended out of the electrode array and were soldered into 0.025 cm thick, 10 cm long electromyogram (EMG) wires (Plastics One, Roanoke, VA). A 100 μm reference wire was implanted into the cerebellum. Electrodes and EMG wires were connected to a Mill-Max micro connector (Mill-Max, Oyster Bay, NY). The impedance of each electrode tip was measured to ensure acceptable signal impedance (≤300 kΩ at 10 KHz) and electrode tips above the desired

resistance were gold plated by pulse-electrolysis with a non-cyanide gold solution (SIFCO ASC, Independence, OH).

Surgery

Anesthesia was performed under isoflurane (Webster Veterinary, Sterling, MA; 2 lt/min O_2, 2% isoflurane). The skull was exposed and four holes (2 for screw anchors and 2 for electrodes) drilled. Two miniature dome-shaped screws were placed above the left parietal cortex and left frontal cortex to provide structural support for the electrodes. The electrode was placed in the hippocampus (AP: −3.8 mm from bregma; ML: 2.0 mm; DV: −1.8 mm). The tip of the electrode bundle is lowered above the CA1 pyramidal cell layer of the hippocampus using a stereotaxic frame (Kopf Instruments, Tujunga, CA). One additional screw was placed on the posterior ridge of the skull to be used as a ground connection. Two EMG wires are threaded into nuchal muscles bilaterally to lie between the two uppermost muscle layers and anchored on the neck with a loose double knot through the superficial layer of the neck muscle using Tricron surgical sutures.

Sleep Scoring

Sleep was scored in animals using a combination of hippocampal EEG and EMG in the nuchal muscles. The EEG signal was band-pass filtered at 1 Hz–35 Hz and the EMG signal was band-pass filtered at 10 Hz – 50 Hz. The EEG signal was also filtered at 1–4 Hz for Delta and 4–12 Hz for Theta oscillatory power calculations. Rats' behavioral states were distinguished at 10 second windows in conjunction with Theta and Delta power calculations derived from filtered signals 10 seconds at a time in conjunction with filtered EMG traces. The awake state was distinguished by movement and low EEG power; the NREM state was determined by a high delta/theta oscillation power ratio and lack of movement; the REM state was identified by low delta/theta oscillation power ratio and loss of muscle tone. Manual scoring of EEG and EMG data were carried out using SleepScorer developed in the laboratory of Dr. Gina Poe (University of Michigan, Ann Arbor, MI) (Gross et al., 2009).

Histology

Animals were deeply anesthetized with urethane (3 mg/kg, i.p.) and a 10mA electrical current is passed through a functioning lead on the electrodes for 20 seconds to mark the electrode position. The animals were then perfused transcardially with 120 mL phosphate buffered saline (PBS: 137 mM NaCl, 2.7 mM KCL, 8.1 mM Na2HPO4 • 2 H2O, 1.76 mM KH2PO4, pH=7.4) followed by 250 mL of sulfide perfusate (Na2S, NaH2PO4 in 250 mL ddH20). Immediately upon harvest, brains were post-fixed in 4% paraformaldehyde for 24h and then in 30% sucrose solution. Coronal sections through the hippocampus were cut at 40 μm. Slices were then mounted and stained with the TIMM staining solution (120 mL Arabic gum (500g Arabic gum in 1000 mL ddH20), 20 mL Citrate Buffer (5.1 g citric acid and 4.7 g sodium citrate in 20 mL ddH20), 60 mL hydroquinone (3.4 g Hydroquinone in 60 mL ddH20), 1 mL silver nitrate (0.17 g silver nitrate in 1 mL ddH20). Every third slice was mounted, dehydrated in ethanol, and stained with cresyl violet. Electrode tracks on the slides were observed for DiI staining in the hippocampus, indicating electrode placement.

Spike Detection

Interictal spikes were visually scored with candidate events occurring whenever the derivative of the hippocampal EEG electrode signal was higher than 5 standard deviations from the mean. The interictal spikes were distinguished from sharp-wave ripples by the lack of a ripple component as well as a 50–100 ms silent period following the interictal spike.

Histological Scoring

Cell layer damage (Table 1) and mossy fiber sprouting (Table 2) was assessed using guidelines previously presented (Liu et al., 1999). Two sections (left and right sided) were scored blindly for each rat using these guidelines in the CA3 and the supragranular regions of the hippocampus. Alternative slices were stained with cresyl violet to assess cell layer damage in the hippocampal regions. Slides stained with cresyl violet were assessed for cell loss in the hilus, CA1 and CA3 subfields of the hippocampus. The severity of cell loss was established using a semi-quantitative scale (Table 1). The mean of the scores were calculated for each animal. Timm staining was analyzed visually using a semi-quantitative scale (Table 2) for terminal sprouting in CA3 and supragranular region. Timm staining in the pyramidal and the infrapyramidal CA3 regions and supragranular region was assessed in each section from the septal area (approximately 3.8 mm posterior to bregma). Assessment of the Timm score in the supragranular region as done in the inferior blade of the dentate. Both hippocampi of the specimens were assessed.

Results

TLE rats have unprovoked temporal lobe seizures

Presence of spontaneous behavioral seizures was confirmed visually in all TLE animals included in the study. All TLE rats (N=10) were observed to have at least one unprovoked stage 3 seizure, consisting of the rat standing on its posterior legs while in status (Racine, 1972), at least 2 weeks after induction to be included in this study. During rest, interictal spikes were observed in TLE rats with an average incidence of 0.62±0.56 /min. No interictal spikes were observed in control rats.

TLE rats have spatial memory impairments

TLE (N=7) and control rats (N=4) were trained to find the platform in the Morris water maze (MWM) task 4 times each day for 4 consecutive days followed by a probe trial on the final day. After adjustment for day of testing, TLE rats were 0.24±0.12 (Cox proportional hazard ratio) times as likely to find the platform compared to controls (Fig. 1a. p=0.003). Additionally, TLE rats spent less time in the target quadrant in the probe trial than controls (Fig. 1b, p=0.04). Automated analysis of video recordings showed no differences in swimming speed between the groups. Thus, TLE rats exhibit marked spatial memory impairments in the MWM task.

TLE rats have mossy fiber sprouting and cell loss in the hippocampus

We stained brain sections from all animals using a Timm and a Cresyl Violet stain for histological study. Cresyl violet staining was carried out on alternate slices. Moderate-to-

severe cell loss (cell layer damage score: 2.21±0.01) was found bilaterally in the CA1 layer of the hippocampus in TLE rats (Table 1, Fig. 2a, c). TLE rats also showed severe mossy fiber sprouting bilaterally in the dentate gyrus (sprouting score: 3.43±0.71) and mild sprouting in the CA3 layer (sprouting score: 0.64±0.26) of the hippocampus (Table 2, Fig. 2b, d). Therefore, impairments in spatial memory performance are accompanied by moderate-to-severe histopathology in the hippocampus in TLE rats.

TLE rats have normal place cell firing and lower spatial fidelity during a repetitive spatial memory task

Single-unit activity (action potentials) was recorded while animals ran in a preferred direction for food reward in a circular track (defined as RUN). TLE rats showed higher direction preference ($p=0.001$) during the experiments. Place cells recorded from TLE rats (Number of rats: N=3; Number of experiments: n=5) exhibited similar firing rate and place field properties to controls (N=3; n=6). Place cells recorded from TLE rats had lower coherence (Fig. 3b. $p=0.025$). These results show that the spatial memory impairments and in TLE rats are reflected at the single-cell level in that place cells recorded from TLE rats exhibit lower spatial fidelity. The proportion of units selected for analysis was not different between the groups ($p=0.24$).

TLE rats have normal sleep macro-architecture

We recorded EEG, single-unit activity, and EMG while the animals slept in their home cages above the circular track immediately after RUN (defined as POST). There were no differences in the average firing rates of place cells (Fig. 4a, $p=0.2214$). TLE rats spent the same proportion of time in each sleep state during POST. There were no differences in the delta- and theta-band power in the local EEG. Overall, we did not find a clear disruption in sleep macrostructure (Fig. 4b) or typical sleep oscillations in TLE rats (Fig. 4c).

Behavior-driven place cell firing patterns are replayed real-time during the subsequent rest period in TLE rats

The temporal structure of place cell activity during behavior was compared to the activity in the sleep period following maze training using a real-time template correlation method. Consensus templates (Fig. 5) were computed for each experiment and were correlated with the cell activity during the sleep period in moving windows. The resulting correlation coefficients (Cts) were then compared to those obtained by correlating the consensus template with the shuffled version of the POST dataset (Fig. 6a). Ct distributions from all experiments were found to be significantly different from their corresponding null distributions (KS test, $p<0.001$). Reactivation of sequences of cell firing was observed in both TLE and control rats as shown by heavier tails of the sample dataset than the 95^{th} percentile of the shuffled dataset (Fig. 6b, $p<0.05$). Z-scored Ct distributions were significantly different between the two groups (Fig. 6a, KS test, $p<0.001$) where a higher incidence of negative correlations were observed in TLE rats ($p<0.001$). Our real-time template correlation results show that real-time reactivation of cell activity patterns in the rest period following behavior is intact in TLE rats.

Behavior-driven sequences of place cell firing are replayed during population bursts in the subsequent rest period in TLE rats

The sequential firing of cells during population bursts was compared to the sequences during behavior using a Markov Chain model (Kincses et al., 2003; Le Cam et al., 2013). To determine whether a high-order sequential structure exists in the neuronal firing, we first computed the block entropies of sequential firing of cells in bursts during sleep where words were divided into blocks of 1–8 symbols (where a symbol is a cell's median firing within a burst). These entropies (scaled by the size of the block, k) are an estimate of the *entropy rate* of the sequence (Cover and Thomas, 1991) and the true entropy rate is the limit as the block size tends to infinity (i.e. the horizontal asymptote of the sequence in Fig. 7a). The curse of dimensionality precludes the experimental determination of block entropies for large block sizes (the number of blocks is exponential in the length of the block), but for modest sized blocks the estimated entropy rate shows a consistent decrease for both groups of animals (Fig. 7a). Our analysis confirmed that sequences extracted from both groups have high-order structure during bursts as evidenced by a steady decrease of the estimated block entropy over word length (Fig. 7a). The incidence probabilities of behavior sequences were consistently higher than the corresponding null distribution obtained by shuffling the dataset, as shown by z-scores that are consistently higher than 1.96 (Fig. 7c). This finding shows that consensus sequences are reactivated more often in the real dataset than the null dataset, providing evidence for reactivation of behavioral sequences of firing during sleep. Thus, the sequences of cell activity encoded during behavior are enriched in sleep-derived Markov models of TLE rats *despite* the marked differences in their hippocampal histology and the degradation in their places fields.

Discussion

The pilocarpine model of TLE closely parallels the human condition with spontaneous temporal lobe seizures, interictal spikes and hippocampal sclerosis (Cavazos et al., 2004; Sharma et al., 2007). The TLE rat hippocampal network generates lower fidelity place field signals with lower coherence in conjunction with spatial memory performance deficits in the water maze task. These single-unit and spatial memory performance deficits are associated with stereotypical histological markers of TLE. In this study, we show that online processing of information, where physiology and behavior are considered in the context of ongoing cognitive load, is markedly impaired in TLE. Although we are not able to comment on whether these deficits are related to seizure rates and/or the prevalence of interictal spikes due to their low prevalence, we show strong evidence that TLE has altered hippocampal network function in this model.

The spatial information processing deficits we observed in TLE rats may precede sequential activity disruptions in memory consolidation during sleep in the hippocampal network, especially when pyramidal cell activity is considered as an ensemble. Following previously reported sleep disruptions observed in the pilocarpine model of TLE (Matos et al., 2012; Matos et al., 2010), we hypothesized that the real-time reactivation structure as well as the replay of behavior-driven sequences of place cells would be disrupted in the subsequent sleep period. Moreover, the low spatial fidelity of place fields, as evidenced by significantly

lower spatial coherence measures, may point to a disruption specifically in the spatial representation by the place cells in TLE. Our study shows that while spatial coding by place cells in the hippocampus is disrupted, temporal coding remains intact. A recent study (Suh et al., 2013) showed that replay in a mouse model of schizophrenia is perturbed despite normal place fields. This finding complements our results and suggests that spatial coding of place cells (i.e., place field size and fidelity) may be governed by a process separate from their temporal coding (i.e., reactivation structure and replay).

Here, we propose that the mechanisms for the integration of place cells into spatial processing networks in TLE rats are intact while the original spatial representation remains unreliable. In fact, a previous report (Tyler et al., 2012) showed that functional network disruptions during behavior in TLE rats are associated with impairments in spatial memory performance for instantaneous (i.e., non-temporally extended) ensemble activity. Thus, even if the replay of place cells during the subsequent sleep period may lead to the successful integration of spatial information into long-term spatial memory, the behavioral performance deficits remain—possibly due to the low fidelity source spatial information. Thus, the disruption of proper encoding of place cells during behavior may lead to the formation of poor long-term spatial representation.

The poor representation of space may also simply be a function of severe cell loss in the CA1 layer of the hippocampus in the TLE rats where the remaining cells may be charged with a higher information load. Another possibility is that although the spatial processing system is largely intact at the single-cell and ensemble level, the processed information is not properly integrated into the spatial processing network, as evidenced by the disruption phase precession of place cells (Lenck-Santini and Holmes, 2008) as well as the poor speed-theta modulation in the hippocampus (Richard et al., 2013).

The real-time template-matching method provides a quantification of the strength of similarity between behavior and sleep activity patterns of place cells. This method provides a measure of real-time reactivation structure where persistence of organized cell activity may be related to underlying functional network structure during sleep. It has previously been reported (Tatsuno et al., 2006) that the output of the template-matching algorithm is sensitive to preprocessing. We controlled for this possibility by comparing simulated RUN data with simulated sleep using this method where an idealized replay sequence was successfully detected. However, the signal-to-noise ratio of the resulting correlation coefficient vector using real data was not sufficiently large to impose an a priori threshold on the dataset. We thus elected to create surrogate datasets by shuffling columns of real data to determine significant strengths of correlations. This approach allowed us to investigate structural similarities between behavior- and sleep-related activities while preserving zero-lag relationships between cells. The correlation strengths obtained from this approach cannot be solely explained by nonspecific patterns of activity by shuffling sleep data while preserving zero-lag cell firing relationships between neurons firing within a 10 ms bin. The preservation of the zero-lag relationships overcomes a potential bias in our analyses not only due to the physiological synchronized depolarization of pyramidal cells during sharp wave events (Buzsaki, 1989; Louie and Wilson, 2001) but also controls for pathological depolarizations during interictal spikes in TLE rats. Although real-time reactivation structure

was detected using this method, the effect barely achieved statistical significance. Previous reports have found this real-time reactivation effect to be similarly weak in correlation strength (Lee and Wilson, 2002; Louie and Wilson, 2001; Ribeiro et al., 2004; Ribeiro et al., 2007). Given the weak correlation between behavior-driven patterns of activity and patterns observed during sleep, it is likely that the networks in the hippocampus only rarely reactivate full sequences. It may be more likely that, given the Hebbian model of synaptic plasticity, groups of neurons ranging from pairs to full sequences are reactivated to aid in the consolidation of behavior-driven patterns. A two-sample KS test yields a significant difference (Fig. 6a, $p<0.001$) between the distributions of z-scored Cts between the two groups of rats where the incidence of negative Cts was increased in TLE rats. Although the biological relevance of this remains uncertain, it is possible that negative correlation indicates the `undoing' of functional relationships between neurons imposed by behavior. There is precedence for this idea in the literature on synaptic downscaling during sleep (Tononi and Cirelli, 2014). Thus, negative Cts may indicate an overactive system in TLE rats for accelerated forgetting observed in patients with epilepsy (Blake et al., 2000) and thus contribute to the spatial memory impairments in TLE rats. Moreover, Barkas et al. (2012) demonstrated accelerated forgetting in rats and humans with TLE. It is possible, then, that the negative correlations point to a potential mechanism for this finding. Further studies are needed to investigate this possibility.

The Bayesian decoding approach (Brown et al., 1998) is a commonly used method in the study of replay (Davidson et al., 2009; Karlsson and Frank, 2009a). Bayesian decoding requires that populations much larger than we were able to record from TLE rats be recorded simultaneously (Carr et al., 2011). In fact, (Brown et al., 1998) and (Zhang et al., 1998) both noted that Bayesian decoding algorithms work optimally with tens of simultaneously recorded neurons. Our implementation of Bayesian decoding on TLE rats yielded poor prediction of the animal's position during performance, indicating that data collected from TLE rats did not have enough power for Bayesian decoding. For example, Karlsson and Frank (2009b) did not consider sharp-wave ripple events with less than 5 cells active in their Bayesian decoding analyses—such thresholding is not possible in our dataset. Thus, the authors utilized a pairwise measure to relate spiking to place field activity (Karlsson and Frank, 2009b). It is also likely that because the place cell activity in our dataset during behavior in TLE rats did not sufficiently span the whole environment, the rat's position cannot be accurately estimated. Moreover, place cells with multiple place fields is a common occurrence in TLE rats (Lenck-Santini and Holmes, 2008; Liu et al., 2003; Zhou et al., 2007). The Bayesian decoder inflates the decoded position probability distribution over all fields detected (Gupta et al., 2010). We elected to use the template-matching method in an effort to preserve the temporal information contained in multi-field place cells, especially in TLE rats.

Due to extensive neuronal loss in TLE rats, the recording of such large populations required for Bayesian decoding remains a technical and technological challenge. Thus, in smaller populations are sampled, pairwise measures have previously been shown to sufficiently identify reactivation (Cheng and Frank, 2008; O'Neill et al., 2006), which parallel the Markov chain method presented in this study. The Markov chain approach represents a

novel perspective that improves upon the pairwise measures due to its inclusion of sequential information in addition to pairwise relationships between cells.

The template-matching method allows us to study structure of activity in TLE rats despite poor spatial precision and thus aids in the understanding temporal structure in this disease state. The replay phenomenon itself is a temporally structured phenomenon in the hippocampus. Because the rat is not receiving primary spatial information from sensory inputs, the dynamics of spiking during sleep are dictated by connectivity in the brain that was imprinted by the *temporal* structure of neuronal firing during behavior. The dynamics of spiking during sleep are dictated by connectivity in the brain that was imprinted by the temporal structure of neuronal firing during behavior. In this study, we show an enrichment of behavior-relevant features in the temporal statistics of sleep firing in both groups. Thus, the temporal features of cell activity are preserved, even though they lack high-fidelity spatial content during behavior.

After we established the presence of reactivation in real-time in TLE rats, we asked whether patterns of reactivation was contained within bouts of population bursts related to high-frequency ripple oscillations, in line with previous reports of replay (Bendor and Wilson, 2012; Davidson et al., 2009; Ji and Wilson, 2007; Lee and Wilson, 2002). Other reports (Born et al., 2006; Molle et al., 2006) have suggested the presence of multi-layered processes both in the oscillatory and the single-unit levels that promote communication between the hippocampus and other brain regions. In this regard, real-time reactivation may represent the underlying functional network activity while replay during bursts may be directly communicated to other brain regions.

In order to study replay, we first asked how much of the information is contained in sequences of cells by calculating block-entropy measurements using our data. We report that a large portion of the information content is captured by first-order Markov Chains evidenced by the substantial drop in block entropy between the first and second symbols (Fig. 7a), but significant information is represented also by higher order models. Due to the curse of dimensionality, we cannot fit high order Markov models because the dimensionality of those models grows exponentially. There may yet be significant differences between the TLE and control rats with regard to their higher order temporal structure, but these differences must be subtle, as there are no clear *qualitative* distinctions between their block entropy curves. The raw values of the entropies calculated (Fig. 7a) are not comparable across animals because they depend on the total number of neurons sampled, which cannot be controlled *a priori*. However, we find that block entropy curves from each experiment decays significantly, indicating temporal structure. Nevertheless, for both groups, knowing the place cell that has just fired is highly predictive of the next place cell to be activated.

Using the first-order Markov Chain model, we discovered that overlapping pairwise relationships between place cells in both TLE and control rats are both significantly enriched for behavior-derived sequences. Thus, not only do both groups have nontrivial temporal structure, but also a first order model of that structure (i.e. a first order Markov chain) is enriched for *behaviorally relevant* sequences. This is to be contrasted with the alternative possibility that, while temporal structure exists in both groups, behaviorally relevant

sequences would only be enriched in, for example, the control group. Using the first-order Markov Chain model, we discovered that overlapping pairwise relationships between place cells in both TLE and control rats are both significantly enriched for behavior-derived sequences. Thus, not only do both groups have nontrivial temporal structure, but also a first order model of that structure (i.e. a first order Markov chain) is enriched for *behaviorally relevant* sequences. This is to be contrasted with the alternative possibility that, while temporal structure exists in both groups, behaviorally relevant sequences would only be enriched in, for example, the control group. This finding is surprising considering the expectation that both disturbances in the macrostructure of sleep and the prevalence of epileptiform activity in sleep (Ferreira et al., 1999; Matos et al., 2010) would disrupt memory consolidation processes. This chain of activity during the bursting activity may sustain long-term firing relationships following Hebbian rules for synaptic plasticity where pairwise firing relationships between neurons dictate their functional connectivity (Hebb, 1949). However, pyramidal neurons in the CA1 layer of the hippocampus are not directly connected where their functional firing relationships may be governed by input from other brain regions and/or sculpted by local interneurons (Chiovini et al., 2010; Ferguson et al., 2013).

The possibility remains, however, that replay in the hippocampus may not be properly communicated to other brain regions in due to the pathological coupling between brain regions in TLE rats perhaps due to seizure activity (Steriade and Amzica, 1994). Although this hypothesis remains speculative, it is reinforced by the previous finding that the hippocampus-prefrontal cortex network is desynchronized in a flurothyl model of seizures in the rat (Kleen et al., 2011).

Another possibility is that while sleep reactivation structure and replay seem to be intact, the TLE rats have disrupted awake replay. As previously shown, awake hippocampal sharp-wave ripples also support spatial memory (Jadhav et al., 2012) where the disruption of SWRs affect spatial memory performance in rats (Ego-Stengel and Wilson, 2010; Girardeau et al., 2009; Nakashiba et al., 2009). Future studies investigating this possibility are needed to further elucidate the spatial memory processing and consolidation mechanisms in TLE rats.

Finally, it is possible that, while there is sequential structure in TLE rats during bursting activity, the sequential structure itself is different between the groups. Our data does not allow for the investigation of this possibility, due to the poor spatial decoding indicated by our implementation of Bayesian decoding.

Our finding that the hippocampus is able to replay behavior-driven patterns of activity during the subsequent sleep period is surprising considering the spatial memory performance deficits, severe cell loss in the CA1 layer of the hippocampus, mossy fiber sprouting in the Dentate Gyrus as well as lower spatial fidelity of place cells during behavior. Although we detected the presence of reactivation in the real-time scale in both groups, we uncovered a more robust reactivation using a first-order Markov Chain model.

While extrapolating data from rats with TLE to humans has limitations, our findings here may have clinical implications. Because of the putative relationship between reactivation of cells and memory consolidation, attempts have been made to increase reactivation in to improve memory consolidation. Targeted memory reactivation during sleep with auditory or olfactory cues that were presented during learning has been shown to improve memory in normal humans (Oudiette and Paller, 2013; Oudiette et al., 2013). In normal rodents, reactivation of place cells is observed when the auditory cue is presented during sleep following an auditory-spatial association behavior task (Bendor and Wilson, 2012). However, it is unlikely that such strategies to enhance reactivation would be effective in individuals with TLE since our data suggest reactivation is not impaired. In fact, given that reactivation is intact in these animals, strategies that improve memory consolidation processes may end up further reinforcing poorly encoded memories and thus further impair performance. Thus, the impairment in spatial memory performance most likely lies in the impaired encoding during behavior. In the case of TLE, increasing reactivation of poorly coded spatial information during sleep is unlikely to be a successful strategy in improving memory.

In summary, we report that real-time reactivation structure as well as hippocampal replay during sleep in TLE rats is intact. This finding points at an online spatial processing deficit in the presence of normal mechanisms for *offline* memory consolidation in TLE rats. Therefore, the hippocampal networks in TLE rats may reinforce poor spatial memory episodes and thus contribute to cognitive impairments observed in this model. Further studies are needed on the potential involvement of sharp-wave ripple associated replay events as well as the how the hippocampal code may be communicated to other brain regions.

Acknowledgments

We thank Drs. Jeremy Barry, Pierre-Pascal Lenck-Santini and Gina Poe for their contributions and support throughout this study.

Grant Information: This work was supported by the NIH Grants NS074450, NS074450 and NS073083 and the Emmory R. Shapses Research Fund and Michael J. Pietroniro Research Fund (awarded to GLH) and R01-NS075249 (awarded to RCS). RCS is supported by Great Ormond Street Hospital Children's Charity.

References

Bazil CW, Walczak TS. Effects of sleep and sleep stage on epileptic and nonepileptic seizures. Epilepsia. 1997; 38(1):56–62. [PubMed: 9024184]

Bendor D, Wilson MA. Biasing the content of hippocampal replay during sleep. Nat Neurosci. 2012; 15(10):1439–44. [PubMed: 22941111]

Bernasconi N, Bernasconi A, Caramanos Z, Antel SB, Andermann F, Arnold DL. Mesial temporal damage in temporal lobe epilepsy: a volumetric MRI study of the hippocampus, amygdala and parahippocampal region. Brain. 2003; 126(Pt 2):462–9. [PubMed: 12538412]

Blake RV, Wroe SJ, Breen EK, McCarthy RA. Accelerated forgetting in patients with epilepsy: evidence for an impairment in memory consolidation. Brain. 2000; 123(Pt 3):472–83. [PubMed: 10686171]

Born J, Rasch B, Gais S. Sleep to remember. Neuroscientist. 2006; 12(5):410–24. [PubMed: 16957003]

Brown EN, Frank LM, Tang D, Quirk MC, Wilson MA. A statistical paradigm for neural spike train decoding applied to position prediction from ensemble firing patterns of rat hippocampal place cells. J Neurosci. 1998; 18(18):7411–25. [PubMed: 9736661]

Buzsaki G. Two-stage model of memory trace formation: a role for "noisy" brain states. Neuroscience. 1989; 31(3):551–70. [PubMed: 2687720]

Carr MF, Jadhav SP, Frank LM. Hippocampal replay in the awake state: a potential substrate for memory consolidation and retrieval. Nat Neurosci. 2011; 14(2):147–53. [PubMed: 21270783]

Cavazos JE, Jones SM, Cross DJ. Sprouting and synaptic reorganization in the subiculum and CA1 region of the hippocampus in acute and chronic models of partial-onset epilepsy. Neuroscience. 2004; 126(3):677–88. [PubMed: 15183517]

Chan S, Baldeweg T, Cross JH. A role for sleep disruption in cognitive impairment in children with epilepsy. Epilepsy Behav. 2011; 20(3):435–40. [PubMed: 21310668]

Cheng S, Frank LM. New experiences enhance coordinated neural activity in the hippocampus. Neuron. 2008; 57(2):303–313. [PubMed: 18215626]

Chiovini B, Turi GF, Katona G, Kaszas A, Erdelyi F, Szabo G, Monyer H, Csakanyi A, Vizi ES, Rozsa B. Enhanced dendritic action potential backpropagation in parvalbumin-positive basket cells during sharp wave activity. Neurochem Res. 2010; 35(12):2086–95. [PubMed: 21046239]

Clifford DB, Olney JW, Maniotis A, Collins RC, Zorumski CF. The functional anatomy and pathology of lithium-pilocarpine and high-dose pilocarpine seizures. Neuroscience. 1987; 23(3):953–68. [PubMed: 3437996]

Cover, TM.; Thomas, JA. Elements of information theory. Wiley; New York: 1991.

Crespel A, Baldy-Moulinier M, Coubes P. The relationship between sleep and epilepsy in frontal and temporal lobe epilepsies: practical and physiopathologic considerations. Epilepsia. 1998; 39(2): 150–7. [PubMed: 9577994]

Crespel A, Coubes P, Baldy-Moulinier M. Sleep influence on seizures and epilepsy effects on sleep in partial frontal and temporal lobe epilepsies. Clin Neurophysiol. 2000; 111(Suppl 2):S54–9. [PubMed: 10996555]

Curia G, Longo D, Biagini G, Jones RS, Avoli M. The pilocarpine model of temporal lobe epilepsy. J Neurosci Methods. 2008; 172(2):143–57. [PubMed: 18550176]

Davidson TJ, Kloosterman F, Wilson MA. Hippocampal replay of extended experience. Neuron. 2009; 63(4):497–507. [PubMed: 19709631]

Dewolfe JL, Malow B, Huguenard J, Stickgold R, Bourgeois B, Holmes GL. Sleep and epilepsy: a summary of the 2011 merritt-putnam symposium. Epilepsy Curr. 2013; 13(1):42–9. [PubMed: 23447740]

Diba K, Buzsaki G. Forward and reverse hippocampal place-cell sequences during ripples. Nat Neurosci. 2007; 10(10):1241–2. [PubMed: 17828259]

Diekelmann S, Born J. The memory function of sleep. Nat Rev Neurosci. 2010; 11(2):114–26. [PubMed: 20046194]

Ego-Stengel V, Wilson MA. Disruption of ripple-associated hippocampal activity during rest impairs spatial learning in the rat. Hippocampus. 2010; 20(1):1–10. [PubMed: 19816984]

Fenton AA, Lytton WW, Barry JM, Lenck-Santini PP, Zinyuk LE, Kubik S, Bures J, Poucet B, Muller RU, Olypher AV. Attention-like modulation of hippocampus place cell discharge. J Neurosci. 2010; 30(13):4613–25. [PubMed: 20357112]

Ferguson KA, Huh CY, Amilhon B, Williams S, Skinner FK. Experimentally constrained CA1 fast-firing parvalbumin-positive interneuron network models exhibit sharp transitions into coherent high frequency rhythms. Front Comput Neurosci. 2013; 7:144. [PubMed: 24155715]

Fernandez IS, Peters JM, Hadjiloizou S, Prabhu SP, Zarowski M, Stannard KM, Takeoka M, Rotenberg A, Kothare SV, Loddenkemper T. Clinical staging and electroencephalographic evolution of continuous spikes and waves during sleep. Epilepsia. 2012; 53(7):1185–95. [PubMed: 22578248]

Ferreira BL, Valle AC, Cavalheiro EA, Timo-Iaria C. Prevalence of epileptic seizures along the wakefulness-sleep cycle in adult rats submitted to status epilepticus in early life. Dev Neurosci. 1999; 21(3–5):339–44. [PubMed: 10575257]

Girardeau G, Benchenane K, Wiener SI, Buzsaki G, Zugaro MB. Selective suppression of hippocampal ripples impairs spatial memory. Nat Neurosci. 2009; 12(10):1222–3. [PubMed: 19749750]

Gross BA, Walsh CM, Turakhia AA, Booth V, Mashour GA, Poe GR. Open-source logic-based automated sleep scoring software using electrophysiological recordings in rats. J Neurosci Methods. 2009; 184(1):10–8. [PubMed: 19615408]

Gupta AS, van der Meer MA, Touretzky DS, Redish AD. Hippocampal replay is not a simple function of experience. Neuron. 2010; 65(5):695–705. [PubMed: 20223204]

Hebb, DO. The organization of behavior; a neuropsychological theory. Wiley; New York: 1949. p. xixp. 335

Herman ST. Epilepsy and sleep. Curr Treat Options Neurol. 2006; 8(4):271–9. [PubMed: 16942670]

Holmes GL, Lenck-Santini PP. Role of interictal epileptiform abnormalities in cognitive impairment. Epilepsy Behav. 2006; 8(3):504–15. [PubMed: 16540376]

Jackson JC, Johnson A, Redish AD. Hippocampal sharp waves and reactivation during awake states depend on repeated sequential experience. J Neurosci. 2006; 26(48):12415–26. [PubMed: 17135403]

Jadhav SP, Kemere C, German PW, Frank LM. Awake hippocampal sharp-wave ripples support spatial memory. Science. 2012; 336(6087):1454–8. [PubMed: 22555434]

Ji D, Wilson MA. Coordinated memory replay in the visual cortex and hippocampus during sleep. Nat Neurosci. 2007; 10(1):100–7. [PubMed: 17173043]

Jokeit H, Luerding R, Ebner A. Cognitive impairment in temporal-lobe epilepsy. Lancet. 2000; 355(9208):1018–9. [PubMed: 10768465]

Karlsson MP, Frank LM. Awake replay of remote experiences in the hippocampus. Nat Neurosci. 2009a; 12(7):913–8. [PubMed: 19525943]

Karlsson MP, Frank LM. Awake replay of remote experiences in the hippocampus. Nature neuroscience. 2009b; 12(7):913–918.

Kincses WE, Braun C, Kaiser S, Grodd W, Ackermann H, Mathiak K. Reconstruction of extended cortical sources for EEG and MEG based on a Monte-Carlo-Markov-chain estimator. Hum Brain Mapp. 2003; 18(2):100–10. [PubMed: 12518290]

Kleen, JK.; Scott, RC.; Lenck-Santini, PP.; Holmes, GL. Cognitive and Behavioral Co-Morbidities of Epilepsy. In: Noebels, JL.; Avoli, M.; Rogawski, MA.; Olsen, RW.; Delgado-Escueta, AV., editors. Jasper's Basic Mechanisms of the Epilepsies. 4th ed. Bethesda (MD): 2012.

Kleen JK, Wu EX, Holmes GL, Scott RC, Lenck-Santini PP. Enhanced oscillatory activity in the hippocampal-prefrontal network is related to short-term memory function after early-life seizures. J Neurosci. 2011; 31(43):15397–406. [PubMed: 22031886]

Le Cam S, Louis-Dorr V, Maillard L. Hidden Markov chain modeling for epileptic networks identification. Conf Proc IEEE Eng Med Biol Soc. 2013; 2013:4354–7. [PubMed: 24110697]

Lee AK, Wilson MA. Memory of sequential experience in the hippocampus during slow wave sleep. Neuron. 2002; 36(6):1183–94. [PubMed: 12495631]

Lenck-Santini PP, Holmes GL. Altered phase precession and compression of temporal sequences by place cells in epileptic rats. J Neurosci. 2008; 28(19):5053–62. [PubMed: 18463258]

Lin H, Holmes GL, Kubie JL, Muller RU. Recurrent seizures induce a reversible impairment in a spatial hidden goal task. Hippocampus. 2009; 19(9):817–27. [PubMed: 19235227]

Liu X, Muller RU, Huang LT, Kubie JL, Rotenberg A, Rivard B, Cilio MR, Holmes GL. Seizure-induced changes in place cell physiology: relationship to spatial memory. J Neurosci. 2003; 23(37):11505–15. [PubMed: 14684854]

Liu Z, Gatt A, Werner SJ, Mikati MA, Holmes GL. Long-term behavioral deficits following pilocarpine seizures in immature rats. Epilepsy Res. 1994; 19(3):191–204. [PubMed: 7698095]

Liu Z, Yang Y, Silveira DC, Sarkisian MR, Tandon P, Huang LT, Stafstrom CE, Holmes GL. Consequences of recurrent seizures during early brain development. Neuroscience. 1999; 92(4): 1443–54. [PubMed: 10426498]

Louie K, Wilson MA. Temporally structured replay of awake hippocampal ensemble activity during rapid eye movement sleep. Neuron. 2001; 29(1):145–56. [PubMed: 11182087]

Lucas MM, Lenck-Santini PP, Holmes GL, Scott RC. Impaired cognition in rats with cortical dysplasia: additional impact of early-life seizures. Brain. 2011; 134(Pt 6):1684–93. [PubMed: 21602270]

Malow BA. The interaction between sleep and epilepsy. Epilepsia. 2007; 48(Suppl 9):36–8. [PubMed: 18047600]

Manns JR, Hopkins RO, Reed JM, Kitchener EG, Squire LR. Recognition memory and the human hippocampus. Neuron. 2003a; 37(1):171–80. [PubMed: 12526782]

Manns JR, Hopkins RO, Squire LR. Semantic memory and the human hippocampus. Neuron. 2003b; 38(1):127–33. [PubMed: 12691670]

Markov, A. Extension of the Limit Theorems of Probability Theory to a Sum of Variables Connected in a Chain. Howard, R., editor. Wiley; New York: 1971. p. 552-577.

Mathern GW, Babb TL, Leite JP, Pretorius K, Yeoman KM, Kuhlman PA. The pathogenic and progressive features of chronic human hippocampal epilepsy. Epilepsy Res. 1996; 26(1):151–61. [PubMed: 8985697]

Matos G, Ribeiro DA, Alvarenga TA, Hirotsu C, Scorza FA, Le Sueur-Maluf L, Noguti J, Cavalheiro EA, Tufik S, Andersen ML. Behavioral and genetic effects promoted by sleep deprivation in rats submitted to pilocarpine-induced status epilepticus. Neurosci Lett. 2012; 515(2):137–40. [PubMed: 22450051]

Matos G, Tsai R, Baldo MV, de Castro I, Sameshima K, Valle AC. The sleep-wake cycle in adult rats following pilocarpine-induced temporal lobe epilepsy. Epilepsy Behav. 2010; 17(3):324–31. [PubMed: 20133208]

Mello LE, Cavalheiro EA, Tan AM, Kupfer WR, Pretorius JK, Babb TL, Finch DM. Circuit mechanisms of seizures in the pilocarpine model of chronic epilepsy: cell loss and mossy fiber sprouting. Epilepsia. 1993; 34(6):985–95. [PubMed: 7694849]

Miller LA, Lai R, Munoz DG. Contributions of the entorhinal cortex, amygdala and hippocampus to human memory. Neuropsychologia. 1998; 36(11):1247–56. [PubMed: 9842769]

Molle M, Yeshenko O, Marshall L, Sara SJ, Born J. Hippocampal sharp wave-ripples linked to slow oscillations in rat slow-wave sleep. J Neurophysiol. 2006; 96(1):62–70. [PubMed: 16611848]

Morris R. Developments of a water-maze procedure for studying spatial learning in the rat. J Neurosci Methods. 1984; 11(1):47–60. [PubMed: 6471907]

Muller RU, Kubie JL. The effects of changes in the environment on the spatial firing of hippocampal complex-spike cells. J Neurosci. 1987; 7(7):1951–68. [PubMed: 3612226]

Nadasdy Z, Hirase H, Czurko A, Csicsvari J, Buzsaki G. Replay and time compression of recurring spike sequences in the hippocampus. J Neurosci. 1999; 19(21):9497–507. [PubMed: 10531452]

Nakashiba T, Buhl DL, McHugh TJ, Tonegawa S. Hippocampal CA3 output is crucial for ripple-associated reactivation and consolidation of memory. Neuron. 2009; 62(6):781–7. [PubMed: 19555647]

Nemenman, I.; Shafee, F.; Bialek, W. Entropy and inference, revisited. 2001. arXiv:physics/0108025

O'Keefe J, Dostrovsky J. The hippocampus as a spatial map. Preliminary evidence from unit activity in the freely-moving rat. Brain Res. 1971; 34(1):171–5. [PubMed: 5124915]

O'Neill J, Senior T, Csicsvari J. Place-selective firing of CA1 pyramidal cells during sharp wave/ripple network patterns in exploratory behavior. Neuron. 2006; 49(1):143–155. [PubMed: 16387646]

Oudiette D, Paller KA. Upgrading the sleeping brain with targeted memory reactivation. Trends Cogn Sci. 2013; 17(3):142–9. [PubMed: 23433937]

Oudiette D, Santostasi G, Paller KA. Reinforcing rhythms in the sleeping brain with a computerized metronome. Neuron. 2013; 78(3):413–5. [PubMed: 23664610]

Racine RJ. Modification of seizure activity by electrical stimulation. II. Motor seizure. Electroencephalogr Clin Neurophysiol. 1972; 32(3):281–94. [PubMed: 4110397]

Ribeiro S, Gervasoni D, Soares ES, Zhou Y, Lin SC, Pantoja J, Lavine M, Nicolelis MA. Long-lasting novelty-induced neuronal reverberation during slow-wave sleep in multiple forebrain areas. PLoS Biol. 2004; 2(1):E24. [PubMed: 14737198]

Ribeiro S, Shi X, Engelhard M, Zhou Y, Zhang H, Gervasoni D, Lin SC, Wada K, Lemos NA, Nicolelis MA. Novel experience induces persistent sleep-dependent plasticity in the cortex but not in the hippocampus. Front Neurosci. 2007; 1(1):43–55. [PubMed: 18982118]

Richard GR, Titiz A, Tyler A, Holmes GL, Scott RC, Lenck-Santini PP. Speed modulation of hippocampal theta frequency correlates with spatial memory performance. Hippocampus. 2013

Scott RC, Richard GR, Holmes GL, Lenck-Santini PP. Maturational dynamics of hippocampal place cells in immature rats. Hippocampus. 2011; 21(4):347–53. [PubMed: 20865725]

Scoville WB, Milner B. Loss of recent memory after bilateral hippocampal lesions. J Neurol Neurosurg Psychiatry. 1957; 20(1):11–21. [PubMed: 13406589]

Sharma AK, Reams RY, Jordan WH, Miller MA, Thacker HL, Snyder PW. Mesial temporal lobe epilepsy: pathogenesis, induced rodent models and lesions. Toxicol Pathol. 2007; 35(7):984–99. [PubMed: 18098044]

Steriade M, Amzica F. Dynamic coupling among neocortical neurons during evoked and spontaneous spike-wave seizure activity. J Neurophysiol. 1994; 72(5):2051–69. [PubMed: 7884444]

Stickgold R. Sleep-dependent memory consolidation. Nature. 2005; 437(7063):1272–8. [PubMed: 16251952]

Stickgold R, Fosse R, Walker MP. Linking brain and behavior in sleep-dependent learning and memory consolidation. Proc Natl Acad Sci U S A. 2002; 99(26):16519–21. [PubMed: 12499518]

Strauss E, Loring D, Chelune G, Hunter M, Hermann B, Perrine K, Westerveld M, Trenerry M, Barr W. Predicting cognitive impairment in epilepsy: findings from the Bozeman epilepsy consortium. J Clin Exp Neuropsychol. 1995; 17(6):909–17. [PubMed: 8847396]

Suh J, Foster DJ, Davoudi H, Wilson MA, Tonegawa S. Impaired hippocampal ripple-associated replay in a mouse model of schizophrenia. Neuron. 2013; 80(2):484–93. [PubMed: 24139046]

Tatsuno M, Lipa P, McNaughton BL. Methodological considerations on the use of template matching to study long-lasting memory trace replay. J Neurosci. 2006; 26(42):10727–42. [PubMed: 17050712]

Tellez-Zenteno JF, Hernandez-Ronquillo L. A review of the epidemiology of temporal lobe epilepsy. Epilepsy Res Treat. 2012; 2012:630853. [PubMed: 22957234]

Tononi G, Cirelli C. Sleep and the price of plasticity: from synaptic and cellular homeostasis to memory consolidation and integration. Neuron. 2014; 81(1):12–34. [PubMed: 24411729]

Tyler AL, Mahoney JM, Richard GR, Holmes GL, Lenck-Santini PP, Scott RC. Functional network changes in hippocampal CA1 after status epilepticus predict spatial memory deficits in rats. J Neurosci. 2012; 32(33):11365–76. [PubMed: 22895719]

Vlooswijk MC, Jansen JF, de Krom MC, Majoie HM, Hofman PA, Backes WH, Aldenkamp AP. Functional MRI in chronic epilepsy: associations with cognitive impairment. Lancet Neurol. 2010; 9(10):1018–27. [PubMed: 20708970]

Walker MP, Stickgold R. Sleep-dependent learning and memory consolidation. Neuron. 2004; 44(1): 121–33. [PubMed: 15450165]

Walker MP, Stickgold R. Sleep, memory, and plasticity. Annu Rev Psychol. 2006; 57:139–66. [PubMed: 16318592]

Walker MP, Stickgold R. Overnight alchemy: sleep-dependent memory evolution. Nat Rev Neurosci. 2010; 11(3):218. author reply 218. [PubMed: 20168316]

Wilson MA, McNaughton BL. Reactivation of hippocampal ensemble memories during sleep. Science. 1994; 265(5172):676–9. [PubMed: 8036517]

Wu CL, Huang LT, Liou CW, Wang TJ, Tung YR, Hsu HY, Lai MC. Lithium-pilocarpine-induced status epilepticus in immature rats result in long-term deficits in spatial learning and hippocampal cell loss. Neurosci Lett. 2001; 312(2):113–7. [PubMed: 11595347]

Zhang K, Ginzburg I, McNaughton BL, Sejnowski TJ. Interpreting neuronal population activity by reconstruction: unified framework with application to hippocampal place cells. Journal of Neurophysiology. 1998; 79(2):1017–1044. [PubMed: 9463459]

Zhou JL, Lenck-Santini PP, Holmes GL. Postictal single-cell firing patterns in the hippocampus. Epilepsia. 2007; 48(4):713–9. [PubMed: 17437414]

Zola-Morgan S, Squire LR, Amaral DG. Human amnesia and the medial temporal region: enduring memory impairment following a bilateral lesion limited to field CA1 of the hippocampus. J Neurosci. 1986; 6(10):2950–67. [PubMed: 3760943]

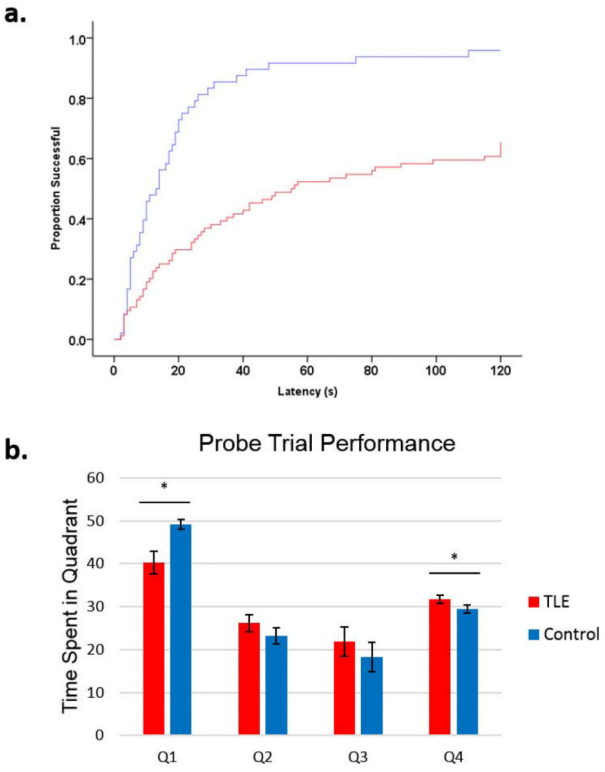

Figure 1.

TLE rats show marked deficits in spatial learning in the Morris Water Maze task. Rats were trained to find the platform in the water maze task 4 times each day for 4 consecutive days followed by a probe trial on the final day. (a) Latency to platform time-to-event curves showing the effect of TLE. The y-axis is the proportion of animals that have reached the platform and the x-axis is latency to platform in seconds. For example, when trials are modeled in, at 60 seconds, ~90% of controls had found the platform while only ~50% of TLE rats had found the platform. When days and trials were modeled using Cox regression model, TLE rats were 0.31±0.11 as likely to find the platform compared to controls.(b) In the probe trial, TLE rats spent less time in the platform quadrant (Q1, p=0.044) and more time in the opposing quadrant (Q4, p=0.001). TLE rats showed several impairments in spatial learning and memory, as was previously shown in this model.

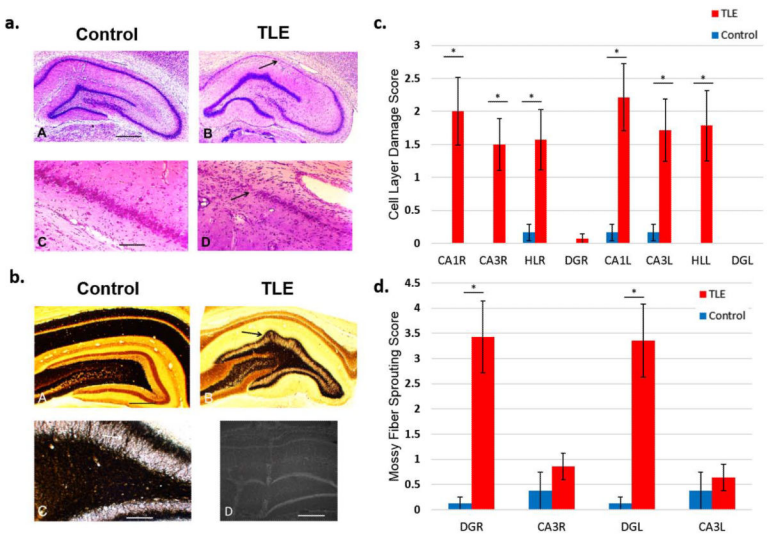

Figure 2.

TLE rats show extensive cell loss and damage in the CA1 and CA3 layers as well as the Hilus (HL) and the Dentate Gyrus (DG) of the hippocampus and mossy fiber sprouting in DG. (a) Cresyl violet staining images. Calibration bar = 1 mm (a), 400 μm (b). Example images of hippocampal regions from TLE and control rats where cell layer damage was assessed. (b) TIMM staining images for assessment of mossy fiber sprouting. Example of mossy fiber sprouting in the hippocampal regions of TLE and control rats (A–C). Electrode placement was confirmed by dipping recording electrodes into fluorescent dye DiI (D). (c) Histological assessment of cell layer damage (Table 1) in the hippocampal regions using Cresyl violet staining. Bilateral cell layer damage in the CA1, CA3, DG, and HL was observed in TLE rats. (d) Histological assessment of mossy fiber sprouting (Table 2) in DG and CA3 regions of the hippocampus using TIMM staining. Bilateral mossy fiber sprouting was present in the DG but not in the CA3 layers. TLE rats were observed to have severe bilateral cell loss in the CA1, CA3 and HL regions as well as extensive bilateral mossy fiber sprouting in the DG. * P <0.001

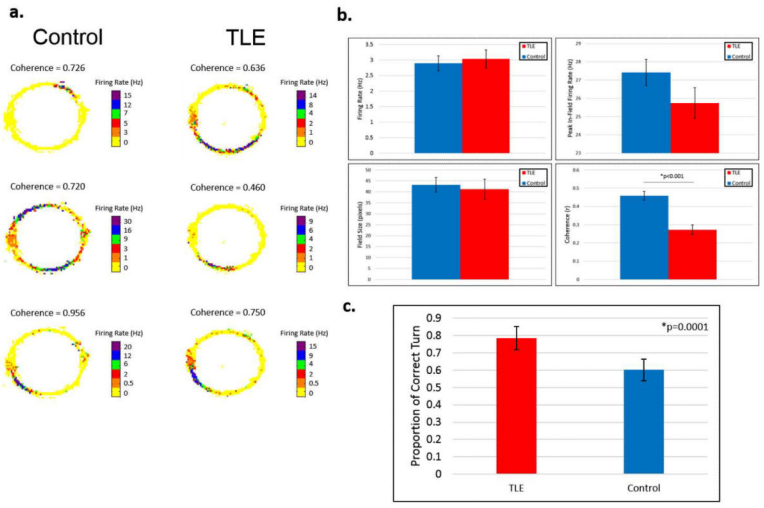

Figure 3.

TLE rats have disrupted place cells. Rats were trained to run in clockwise or counter-clockwise direction in a circular track for food reward on one end (9 o'clock on rate maps). (a) Rate maps are obtained by overlaying unit firing rates recorded from tetrodes in the CA1 layer of the hippocampus with position data recorded from LEDs placed on the animals' headstages. The heat maps show examples of rate maps of place cells recorded from different TLE rats and control rats. (b) Place cells from TLE and Control rats had similar firing rates as well as peak in-field firing rates during the RUN session. There were no differences in average field sizes. Coherence values are calculated by comparing the rate of firing of each pixel to its neighboring pixels (1 pixel = ~1 cm^2) to quantify how smoothly each place cell increases its rate of firing towards the center of its place fields. TLE rats showed lower coherence than controls (GEE, p=0.004). (c) Position data was used to determine rats' behavior in the maze. Each complete turn was considered a correct turn. Only completed turns were included in the analysis. TLE rats showed a higher direction preference than controls (GEE, p=0.0001). Place cells recorded from TLE rats showed decreased coherence that parallel spatial learning and memory deficits discussed previously. TLE rats showed higher directional preference in the repetitive task, suggesting a higher persistence or a lack of behavioral flexibility.

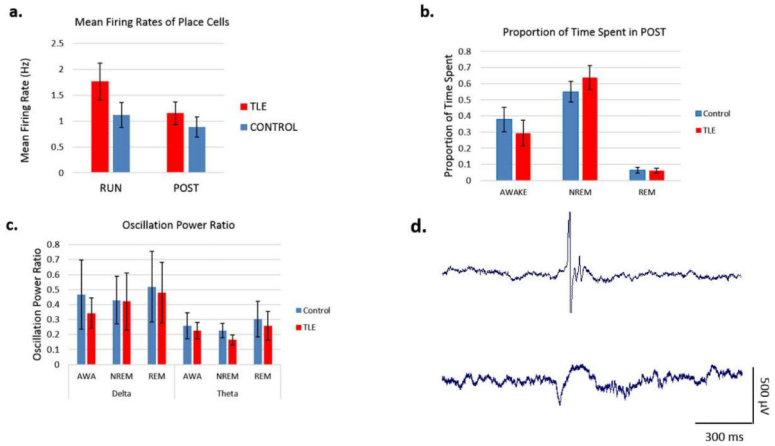

Figure 4.

Sleep macrostructure, oscillatory and single-unit firing characteristics in TLE rats. (a) Place cells recorded from TLE rats showed similar mean firing rates as controls. (b) TLE rats spent slightly, albeit statistically insignificantly, more time in NREM sleep and less time awake during the 1 h recording period in POST. (c) There were no differences in oscillatory power in the Delta or Theta bands during any of the states in POST. (d) Representative examples of an interictal spike (top) and a sharp-wave-ripple event (bottom) from a TLE rat.

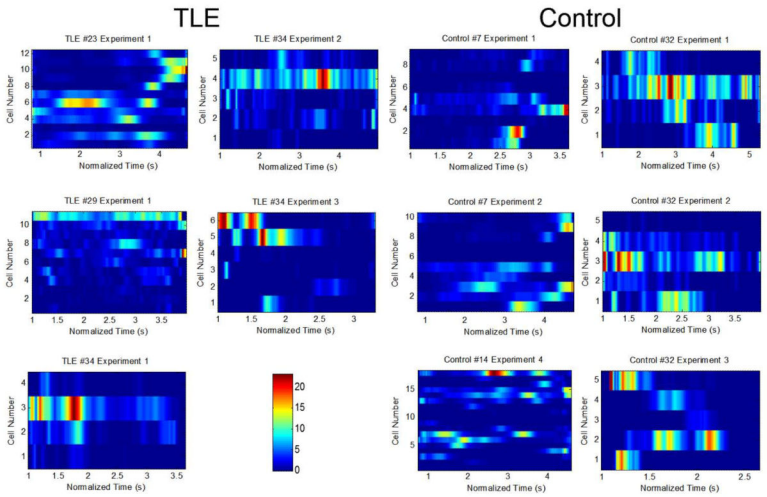

Figure 5.

Consensus templates are calculated to represent overall cell firing during behavior. Heatmaps of unit firing during correct turns over normalized time. The heatmaps on the left panel are obtained using data from TLE rats; the heatmaps on the right panel are obtained from units recorded from control animals. The y-axis is cell number. The x-axis is normalized time in seconds. The heatmaps (referred to as consensus templates) represent the typical activity tendencies of each unit over time. Consensus templates for each experiment were constructed by aligning all correct turns over a normalized time period of 3±1.5 s. These templates were then used to correlate unit activity patterns during behavior with the sleep period to investigate reactivation. Following this method, we extracted an overall heatmap of cell activity to be used both for template correlation and Markov Chain analysis methods. Some place cells were found to fire in multiple normalized fields in the consensus templates. This phenomenon was also observed in place cell rate maps.

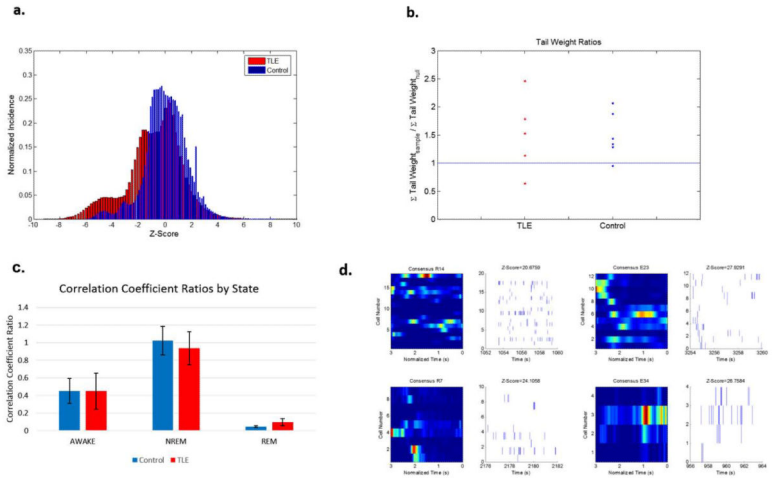

Figure 6.

No differences in temporal structure was observed between TLE and control rats. (a) Z-score histograms of the normalized Ct's for each group in different states during POST. The y-axis is normalized incidence. The x-axis is the z-score obtained using the corresponding shuffled dataset. The inset is zoomed-in to the tails of the distributions for each respective state Ct histogram. (b) Tail weights comparing the z-scores of experiments compared to their corresponding null distributions for each state in POST. The 95th percentile tails of each experiment was compared to its corresponding null distribution by calculating the area under the histogram curves. The y-axis is the area under the histograms obtained from the z-scores in experiments (sample) divided by that calculated from the null distribution. Results are presented as grouped data. Both controls and TLE rats show statistically significant reactivation patterns (where $\sigma_{sample}/\sigma_{null}>1$) during POST. (d) Representative reactivation events (right panels) as defined by maximum z-scores against the surrogate datasets compared with consensus sequences (left panels) from 2 TLE and 2 control rats.

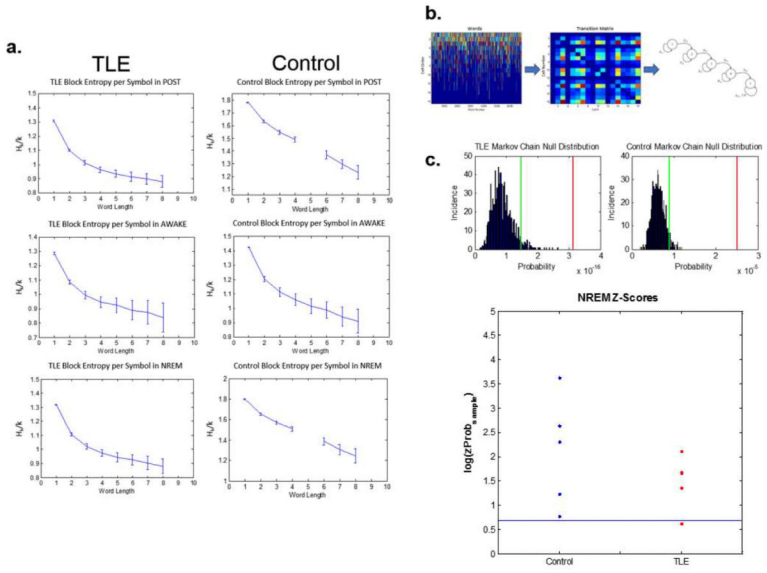

Figure 7.

Sequences of unit firing during behavior is reactivated during POST in both TLE and control rats. (a) Examples of block entropies calculated using words during different states in POST. Left panel: Example TLE rat. Right panel: Example control rat. The y-axis is the block entropy per symbol (H_k/k), The x-axis is the word length. Block entropy analysis revealed high-order sequential structure in both the control and the TLE datasets—i.e., the higher the number of cells fired, the more accurately the model predicts the upcoming cell firing. (b) Markov Chain modeling methods. Left panel: the y-axis is the number of units firing within a word. The x-axis is the word number. Middle panel: transition matrix constructed using pairs of cells firing in sequence. Right panel: Adjacency matrix describing the transitions between unit pairs that result in the behavior sequence. Spike trains from cells are grouped into words separated by 100 ms of silent periods with no unit firing. Sequences within words are obtained by ranking cells by their median timestamps, calculated by the activity of each cell within a word. These sequences are then converted into an adjacency matrix to describe the transitions between pairs of cells (Equation 2). (c) Top panel: Example histograms of Markov Chain null distributions. Green lines denote the 95th percentiles of the null distributions. Red lines show the probability of observing the behavior sequence in the sample dataset. Null distributions are obtained by shuffling unit sequences 1000 times while preserving word lengths. Bottom panel: Z-scores describing the probability of finding the behavior sequence in the sample dataset during NREM sleep calculated using the null distributions obtained from the corresponding shuffled dataset. The consensus sequences were significantly more likely to be observed in the real dataset compared to the shuffled null dataset in both groups, indicating a preference for behavior sequences during the NREM sleep period in POST. Taken together, we show that TLE and control rats both preserve sequential structure of the firing patterns during behavior in the rest period following behavior across all states.

Table 1

Scoring Guidelines for Cell Loss in CA1, CA3 and Hilus

Score	Criteria
0	No cell loss
1	Minimal cell loss
2	Moderate cell loss with preservation of the general cellular architecture with some normal cellular elements.
3	Complete disruption of the normal cellular architecture.

Table 2

Scoring Guidelines for Mossy Fiber Sprouting

Score	Criteria
0	No granules in the along the sub-region
1	Occasional granules in discrete bundles
2	Occasional to moderate granules
3	Prominent granules
4	Highly-concentrated granules in near-continuous distribution
5	Continuous or near-continuous dense laminar band of granules